Design of parallel transmission pulses in the presence of RF errors

Adrian Martin[1], Bastien Guerin[2], Yigitcan Eryaman[2,3], Joaquin L Herraiz[3], Borjan Gagoski[4], Elfar Adalsteinsson[5,6], Lawrence L. Wald[2,6], and Emanuele Schiavi[1]
[1]Applied Mathematics, Universidad Rey Juan Carlos, Mostoles, Madrid, Spain, [2]Radiology, Martinos Center, Massachusetts General Hospital, Charlestown, Massachusetts, United States, [3]Madrid-MIT M+Vision Consortium in RLE, Massachusetts Institute of Technology, Cambridge, Massachusetts, United States, [4]Fetal Neonatal Neuroimaging & Developmental Science Center, Boston Children's Hospital, Harvard Medical School, Boston, Massachusetts, United States, [5]Electrical Engineering and Computer Sciences, Massachusetts Institute of Technology, Cambridge, Massachusetts, United States, [6]Health Sciencies and Technology, Massachusetts Institute of Technology, Cambridge, Massachusetts, United States

Target audience: RF engineers and MR physicists.

Purpose: Parallel transmission RF pulse design has recently addressed the management of global [1] and local SAR [2-5]. None of these methods take into account errors in the transmit chain (see **Fig. 1**) that can cause local SAR to be above safety limits in real life scenarios [6]. We propose a method that uses information about transmit chain fidelity to design pTx pulses that satisfy SAR limits even in the worst case where these errors add up to create the largest possible increase in local and global SAR.

Methods: Measurement of RF chain errors: We measured deviations between pulses as prescribed in the pulse sequence and actually played on a 7T 8-channel pTx system (Siemens, Erlangen GE) as explained in [7]. We did this for a 4-spoke pulse (64 TRs, max. voltage=61.58V) and a saturation pulse (64 TRs, max. voltage=60.45V). Amplitude and phase error histograms are shown in Fig. 1. SAR-robust pTx pulse design: SAR constraints are expressed as quadratic forms inequalities of the form $\boldsymbol{b}^H\boldsymbol{S_i}\boldsymbol{b}<\boldsymbol{SAR_{MAX}}$, $\boldsymbol{b}$ being the designed pulse, $\boldsymbol{S_i}$ being the SAR matrices or their compressed representation using the virtual observation points (VOP) algorithm [8] and $\boldsymbol{SAR_{MAX}}$ being the maximum SAR allowed. We computed SAR-constrained pTx pulses that are safe with respect to RF errors as follows (**Fig. 2**): STEP #1: We calculated an initial pulse $\boldsymbol{b_0}$ using an algorithm that achieves the best flip-angle excitation while explicitly constraining global and local SAR as well as power on every channel [2]. STEP #2: We computed a new pulse $\boldsymbol{b}$ for each $\boldsymbol{S_i}$ reaching the worst possible local and global SAR ($\boldsymbol{SAR_{WC}}$) associated with the initial pulse $\boldsymbol{b_0}$ and consistent with the known accuracy of the RF transmit chain in both amplitude (ε is the maximum amplitude error expressed in percentage of the desired RF voltage) and phase (δ is the maximum phase deviation expressed in degrees) by solving the following constrained convex optimization problem:

$$\boldsymbol{max_b \frac{1}{N_t}\sum_t b^H(t)S_i b(t)\ \ s.t.\,\forall t\ \big||b|-|b_0|\big| \le \varepsilon\,|b_0|\,,|\angle b-\angle b_0| \le\ \delta}.$$

STEP #3: If $\boldsymbol{SAR_{WC}}$ was above the local SAR or global limit, we calculated a new pulse $\boldsymbol{b_0'}$ with a reduced SAR constraint. We used this strategy for the design of 45 degrees flip angle magnitude least-squares (MLS) spokes pulses with a 10% duty-cycle. EM simulation: We tested our approach using simulated data for a 3T body coil with 8 Tx channels and a 7T head array with 8 channels. We used a co-simulation strategy based on the field simulator HFSS and the circuit simulator ADS [9,10]. SAR matrices were computed using the coil electric fields and were compressed in a reduced set of VOPs [8].

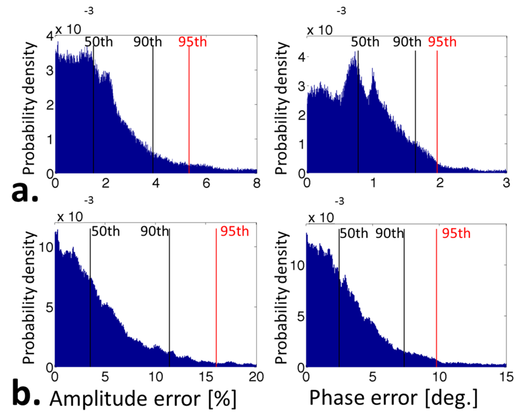

Fig.1. Histograms of magnitude and phase RF errors for a spokes (**a**) and a saturation pulses (**b**). Vertical lines indicate the position of the 50th, 90th and 95th percentiles.

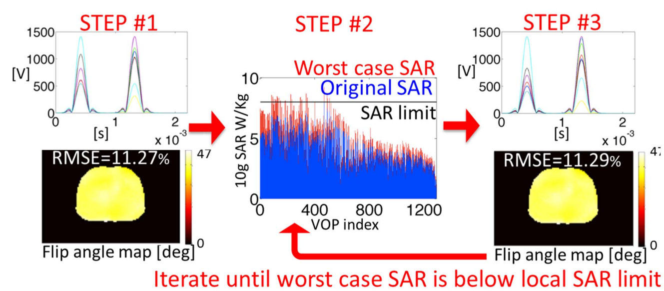

Fig. 2. Flowchart of the robust pulse design process. A first pulse is designed while constraining SAR to the user-defined limit (Step 1). The worst case SAR (SAR_{WC}) for every location (VOP) is then calculated for given maximum RF chain errors (Step 2). If SAR_{WC} exceeds the SAR limit a new pulse is designed with reduced SAR constraint (Step 3)..

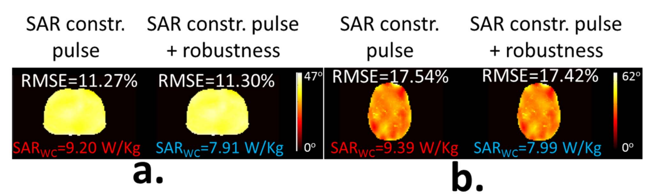

Fig. 3. Flip angle maps for 2-spokes pulses designed at 3T in the body (**a**) and at 7T in the head (**b**).

Results/Discussion: The error distribution of the RF transmit chain were greater (in amplitude and phase) for the saturation pulse than for the spokes pulse (**Fig. 1**). This is likely due to high frequency contents of the saturation pulse that are difficult to reproduce accurately (the spoke pulse was smoother). Based on this data, we used maximum deviations for the amplitude and phase of RF waveforms of 5% and 2.5°. We conclude that enforcing a more restrictive local SAR limit to ensure safety given RF transmission errors did not degrade the flip-angle map dramatically for the spokes pulses, duty cycle, flip angle and SAR limits considered in this study. In the example of **Fig. 3b**, the RMS error even decreased slightly with the SAR limit. This is related with the existence of local minima for the non-convex MLS pulse design optimization problem.

Acknowledgements: Project TEC2012-39095-C03-02 of the Spanish Ministry of Economy and Competitiveness. R01EB006847. Siemens-MIT CKI Alliance. This project is also supported by the Comunidad de Madrid and the Madrid MIT M+Vision Consortium.

References: [1] Zhu Y (2004). MRM **51**(4): 775-784. [2] Guerin B (2013). MRM DOI: 10.1002/mrm.24800. [3] Brunner D (2010). MRM **63**(5): 1280-1291. [4] Lee J (2012). MRM, **67**(6): 1566-1578. [5] Sbrizzi, A. (2012). MRM **67**(3): 824-834. [6] Martin, A. (2013). Proc. ESMRMB **2013**: 69-70. [7] Gagoski, B. (2011). Proc. ISMRM **19**: 3848. [8] Eichfelder, G. (2011). MRM **66**(5): 1468-1476. [9] Guerin B (2013). Proc. ISMRM **21**: 2741. [10] Kozlov, M. (2009) J. Magn. Reson. **200**(1):147-152.